Sodium channels amplify spine potentials

Roberto Araya*†, Volodymyr Nikolenko*†, Kenneth B. Eisenthal‡§, and Rafael Yuste*†§

*Howard Hughes Medical Institute and Departments of †Biological Sciences and ‡Chemistry, Columbia University, New York, NY 10027

Contributed by Kenneth B. Eisenthal, June 11, 2007 (sent for review January 25, 2007)

Dendritic spines mediate most excitatory synapses in the brain. Past theoretical work and recent experimental evidence have suggested that spines could contain sodium channels. We tested this by measuring the effect of the sodium channel blocker tetrodotoxin (TTX) on depolarizations generated by two-photon uncaging of glutamate on spines from mouse neocortical pyramidal neurons. In practically all spines examined, uncaging potentials were significantly reduced by TTX. This effect was postsynaptic and spatially localized to the spine and occurred with uncaging potentials of different amplitudes and in spines of different neck lengths. Our data confirm that spines from neocortical pyramidal neurons are electrically isolated from the dendrite and indicate that they have sodium channels and are therefore excitable structures. Spine sodium channels could boost synaptic potentials and facilitate action potential backpropagation.

dendritic spines | membrane potential | neurons

As predicted by Ramón y Cajal (1), in the mammalian cortex, most synaptic contacts in pyramidal cells are made on dendritic spines (2). Thus, it is natural to wonder whether spines influence synaptic transmission. Indeed, theoretical work over the last six decades has explored the possibility that spines have an electrical function, filtering and/or perhaps amplifying synaptic potentials (3–10). At the same time, other calculations have argued that spines cannot have an electrical function, serving merely as biochemical compartments (11–13). This debate has been reopened by two-photon calcium imaging data that demonstrated that spines have voltage-sensitive calcium channels (14, 15). Therefore, it becomes possible that spines could also have other types of voltage-gated channels, including sodium and potassium channels, and, if so, that spines could be excitable structures (5, 16).

In our recent studies, we have encountered evidence consistent with the existence of sodium channels in the spine. First, numerical simulations indicated that the measured densities of sodium channels in dendritic shafts are too low to sustain action potential (AP) back propagation in pyramidal neurons, and that additional sodium channels are likely to be present in spines to ensure effective back propagation (17). Also, optical measurements of membrane potential using second harmonic generation have shown that backpropagating APs invade spines without a significant decrement in amplitude (18). At the same time, we have found that the spine neck provides a barrier to the propagation of membrane potentials (19), so the full-blown backpropagating AP, rather than invading passively, could be locally generated at the spine. Together, these data suggest that sodium channels might exist in spines, and that they could help promote AP backpropagation.

We have tested this hypothesis by using two-photon uncaging of glutamate to activate spines individually and examine whether their responses are affected by tetrodotoxin (TTX), a specific sodium channel blocker. We find that TTX reduces the amplitude of uncaging potentials in spines but not in dendritic shafts or voltage-clamped neurons. This effect is strong and occurs in spines with different neck lengths and with uncaging potentials of different amplitudes. Our results imply that spines have sodium channels that amplify membrane potentials.

Results

TTX Reduces the Amplitude of Spine-Uncaging Potentials. We tested the hypothesis that spines contain functional sodium channels by characterizing their response to glutamate in the presence or absence of TTX. To activate spines, we used two-photon uncaging of 4-methoxy-7-nitroindolinyl glutamate (20, 21) in basal dendrites from layer 5 pyramidal neurons from slices of mouse visual cortex (Fig. 1*A*). To minimize dendritic filtering, we chose to work with spines that are relatively close (<100 μm) to the soma. As in our recent work (19, 22), we measured the somatic membrane potential in response to uncaging events (4-msec duration), using whole-cell recordings in current clamp. These somatic responses ("uncaging potentials") ranged from ≈0.3 to 1.2 mV and from ≈40 to 300 msec in duration (Figs. 1*B* and 2; amplitude 0.72 ± 0.04 mV, duration 124 ± 9 ms; $n = 76$ spines). On a single spine, the amplitude of the uncaging potential was constant for up to 32 rounds of uncaging (maximum number tested), although the response showed some variability from trial to trial (linear regression fit, slope = 0.007; $P = 0.9$). Also, the response amplitude was constant over periods of at least 5 min ($P = 0.8$, $n = 3$). Depolarizing responses after uncaging pulses only occurred close to the spine head membrane. Uncaging potentials were not detectable if the uncaging laser was located at >1-μm distance from the spine head membrane, as reported (19), indicating that uncaging events were restricted locally to a single spine.

To test whether sodium channels contributed to uncaging potentials, we uncaged glutamate in spines under control conditions (i.e., in standard artificial cerebrospinal fluid) and then repeated the uncaging protocol in the same spine after bath application of TTX (Figs. 1*B* and 2). Bath application of TTX (1 μM) reduced uncaging potentials by 31.6 ± 3.8% in amplitude and by 46.9 ± 4.9% in area (Figs. 1*B*, 2 *A1–A3* and *B*; $n = 19$ spines from eight neurons; *t* test, $P < 0.001$ for average reductions in amplitude and area). Average amplitudes in control spines changed from 0.8 ± 0.05 mV to 0.5 ± 0.03 mV after addition of TTX, and the distribution of the uncaging potentials was shifted to smaller amplitudes (Fig. 2*C1*; $n = 310$ and 308 individual uncaging events in control and TTX, respectively; *t* test, $P < 0.001$, for all individual events). Similarly, the average area of the uncaging events changed from 0.083 ± 0.01 mV sec to 0.042 ± 0.006 mV sec after adding TTX (*t* test, $P < 0.001$, for all individual events). On individual spines, the TTX-dependent amplitude and area reduction ranged from 0 to 62% and from 0 to 70%, respectively, and only 2 of 19 spines showed no apparent TTX sensitivity. In addition, analyses from all spines recorded in TTX (including spines where uncaging potentials were recorded only in control conditions or TTX), also demonstrated a reduction of average uncaging potential amplitudes

Author contributions: R.A. and V.N. contributed equally to this work; R.A., V.N., K.B.E., and R.Y. designed research; R.A. and V.N. performed research; R.A., V.N., K.B.E., and R.Y. analyzed data; and R.A., V.N., K.B.E., and R.Y. wrote the paper.

The authors declare no conflict of interest.

Freely available online through the PNAS open access option.

Abbreviations: AP, action potential; TTX, tetrodotoxin.

§To whom correspondence may be addressed. E-mail: kbe1@columbia.edu or rmy5@columbia.edu.

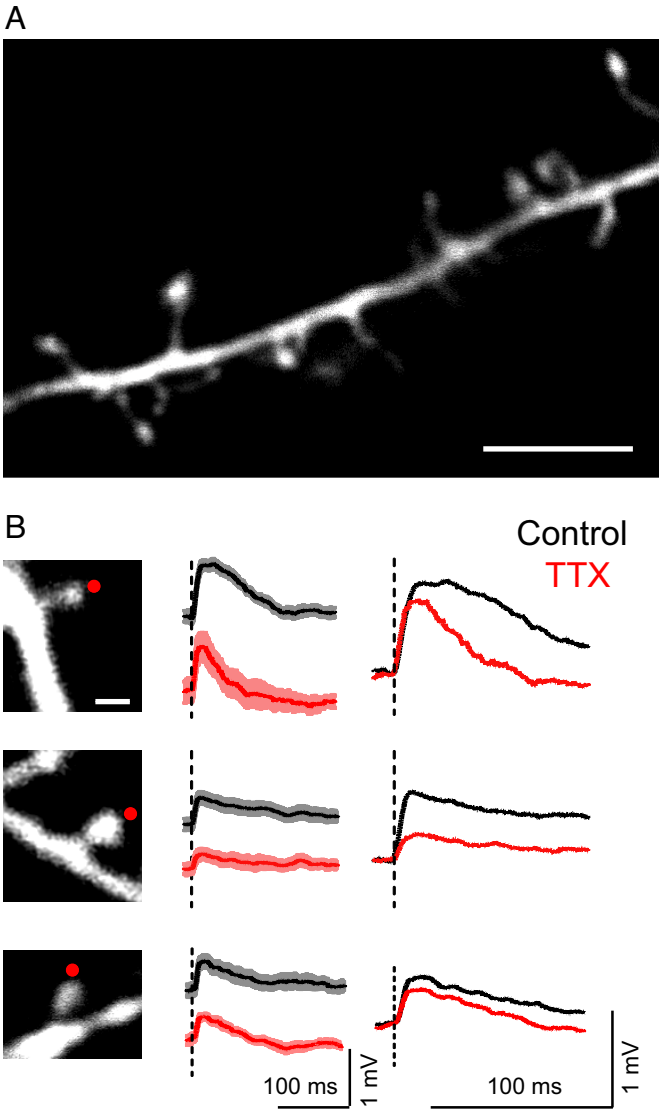

Fig. 1. TTX reduces spine uncaging potentials. (*A*) Representative basal dendrite selected for uncaging from a layer 5 pyramidal neuron, filled with Alexa 488. (Scale bar, 5 μm.) (*B*) Representative spine uncaging experiments. (*Left*) Red dots indicate site of uncaging. (*Center*) Uncaging potentials under control conditions (black traces) and in TTX (red traces) in current clamp configuration. Dashed line is time of uncaging onset. Thicker traces are average of 10–15 depolarizations, and shaded areas illustrate ± SEM. (*Right*) Superimposition of average uncaging potentials. Note how TTX attenuates spine uncaging potentials. (Scale bar, 1 μm.)

(control spines 0.72 ± 0.04 mV, $n = 76$ spines, 31 neurons; spines in TTX: 0.52 ± 0.02 mV, $n = 48$ spines, 11 neurons, t test, $P < 0.001$).

Effect of TTX Is Postsynaptic. We then sought to identify the location of the sodium channels involved in the reduction of uncaging potentials by TTX. We first examined whether the channels were pre- or postsynaptic. Given that the two-photon uncaging volume is larger than the size of a typical synapse of a mouse layer 5 pyramidal neurons (19, 21, 23, 24), glutamate uncaging could indirectly activate presynaptic glutamate receptors (25), which could then release glutamate from the presynaptic terminal and indirectly activate the spine. In this scenario, the sodium channels involved in the amplification of uncaging potentials would be presynaptic.

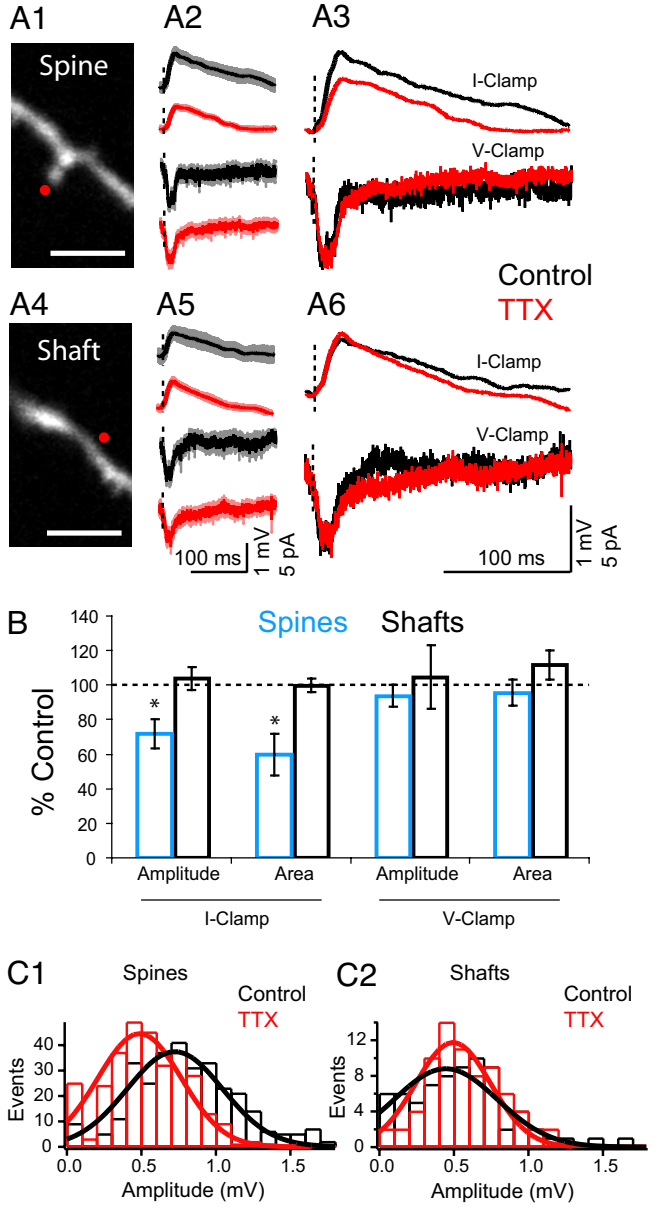

Fig. 2. The effect of TTX is postsynaptic and restricted to spines. (*A*) Uncaging experiments in spine (*A1–A3*) or shaft (*A4–A6*) locations, under control conditions (black traces) and TTX (red traces) in current (top in *A2*, *A3*, *A5*, and *A6*) and voltage clamp (bottom in *A2*, *A3*, *A5*, and *A6*) configurations. (Scale bar, 3 μm.) Note lack of effect of TTX on spine voltage–clamp uncaging events and on shaft uncaging. (*B*) Uncaging potential amplitude and area (percentage from control) after TTX perfusion in spines (blue) and shafts (black), under current– and voltage–clamp configurations. *, $P < 0.01$. (*C*) Histogram of all individual uncaging potentials on spines (*C1*) and shafts (*C2*) in control and TTX. Note a shift toward smaller potentials caused by TTX in distribution of spine, but not shaft potentials.

We tested this by performing TTX experiments in spines recorded under both current and voltage clamp (Fig. 2 *A* and *B*) because the voltage clamp should prevent the activation of postsynaptic sodium channels. To maximize voltage clamp, we performed these experiment in short-necked spines <60 μm away from the soma. In these spines, when measured in current clamp, we observed a significant reduction in amplitude and area of the recorded uncaging potentials when TTX was applied (Fig. 2 *A1–A3* top and *B*; amplitude: 71.6 ± 8.5% of control, t test $P < 0.005$; area, 59.4 ± 12% of control; t test, $P < 0.001$). However,

when the same spines were examined in voltage clamp, TTX did not change the amplitudes or areas of uncaging currents (Fig. 2 *A1–A3* bottom and *B*; amplitude, 93.8 ± 6.2% of control, *t* test, $P = 0.38$; area, 95.4 ± 7.5% of control, *t* test, $P = 0.7$; average currents, ≈7 pA in amplitude and ≈0.18 pA sec in area; $n = 8$ spines, 5 neurons). These results indicate that the sodium channels were located postsynaptically because presynaptic sodium channels should be unaffected by the postsynaptic voltage clamp.

Shaft Uncaging Potentials Are Unaffected by TTX. We then examined whether the sodium channels involved in the amplification were located in the spine or in the dendritic shaft. This latter possibility could be likely, given that layer 5 pyramidal neurons have dendritic sodium channels (26). We tested this by examining the effect of TTX on uncaging potentials generated in dendritic shafts, at locations separated at least 2 μm from any neighboring spine (Fig. 2*A4*). Uncaging potentials in shafts had an amplitude of 0.54 ± 0.08 mV ($n = 5$) and were also stable over time (linear regression fit with slope of −0.007 and $P = 0.55$), but, in contrast to spine uncaging potentials, were much less sensitive to TTX (Fig. 2 *A5* and *A6* top). Specifically, the perfusion of TTX did not change the average amplitude or area of shaft potentials (Fig. 2*B*; control amplitude, 0.54 ± 0.08 mV, TTX amplitude, 0.56 ± 0.09 mV; control area, 0.037 ± 0.009 mV sec; TTX area, 0.032 ± 0.009 mV sec; control, amplitude, 103.9 ± 6.7% of control, *t* test, $P = 0.56$; area, 99.8 ± 3.9% of control, *t* test, $P = 0.95$; $n = 5$ locations) and also did not significantly change their amplitude distributions (Fig. 2*C2*; $n = 72$ and 74 individual uncaging events in control and TTX; $P = 0.54$). Similar results were found under voltage clamp (Fig. 2 *A5* and *A6* bottom), where glutamate uncaging onto shafts in TTX showed no statistical difference in average amplitude or integral values from control uncaging currents (Fig. 2*B*; amplitude, 104.5 ± 18.4% of control; *t* test, $P = 0.81$; area, 111.5 ± 8.4% of control, *t* test, $P = 0.2$). Thus, the sodium channels responsible for the amplification of the spine potential could not be located in the dendritic shaft or the somatic compartments of the neuron, because, otherwise, shaft uncaging potentials should have been similarly affected by TTX. Therefore, we concluded that the sodium channels responsible for the amplification of spine potentials must be located in the spine itself.

TTX Affects Uncaging Potentials of Different Amplitudes. Sodium channels have strong nonlinear voltage dependency (27), so if a larger depolarizations impinged on the spine, they could become more activated. To study the amplitude-dependence of the amplification, to generate larger uncaging potentials, we increased the duration of the uncaging pulse to 10 msec (Fig. 3). In these conditions, depolarizing responses after uncaging pulses still only occurred close to the spine head membrane (Fig. 3 *A1* and *A2*). Already at ≈2 μm away from the spine head, membrane depolarizations were hardly detectable (Fig. 3*A2*), indicating that uncaging events were restricted locally. Thus, the spatial resolution of 10-msec uncaging protocols was still adequate to probe individual spines and not significantly contaminated by glutamate spillover from the uncaging source.

As expected, the amplitude of uncaged excitatory postsynaptic potentials depended on the duration of the uncaging pulse. Prolonging the duration of the uncaging pulse from 4 to 10 msec increased the amplitude of the resulting uncaging potentials (4 msec, amplitude 0.72 ± 0.04 mV, duration 124 ± 9 msec; $n = 76$ spines; 10 msec, amplitude 2.9 ± 0.28 mV, duration 130 ± 14 ms, $n = 15$ spines; $P < 0.001$). This increase is larger than one would expect from a linear dependency on the amount of glutamate released. Thus, it could reflect an increased activation of sodium channels.

To test this, in a subset of spines, we measured these larger uncaging potential before and after addition of TTX. As with the 4-msec potentials, the 10-msec uncaging potentials were reduced by 40.1 ± 6.4% in amplitude and 31.8 ± 5.9% in area by the addition of TTX (Fig. 3 *B1 Inset* and *C1*), which also shifted the distribution to smaller amplitudes of individual uncaging potentials (Fig. 3*B1*). Average amplitudes in control spines changed from 2.5 ± 0.07 mV to 1.3 ± 0.05 mV after addition of TTX, and average areas from 0.3 ± 0.06 to 0.2 ± 0.03 mV sec in TTX ($n = 97$ control potentials and 129 in TTX; $n = 8$ spines from eight neurons; $P < 0.001$ for both amplitude and area). This reduction is comparable to that observed with 4-msec uncaging pulses (Fig. 3*C1*, $P = 0.2$).

We then explored whether TTX had any effect on larger depolarizations in the shaft, using 10-msec uncaging pulses in dendritic shafts (82 uncaging events in control vs. 96 in TTX from $n = 4$ shaft locations). As with 4-msec protocols, 10-msec shaft uncaging potentials were similar in amplitudes and areas before and after the addition of TTX (Fig. 3 *B2* and *C1*; amplitude: 1.4 ± 0.06 mV vs. 1.4 ± 0.06 mV for control and TTX, respectively; area, 0.09 ± 0.02 mV sec, vs. 0.089 ± 0.017 mV sec for control and TTX, respectively; $n = 4$ shaft locations, $P = 0.8$).

Finally, we inquired whether the amount of sodium channel amplification was correlated with the amplitude of the uncaging potential. For this analysis, we incorporated all data, pooling experiments performed with 4- and 10-msec uncaging potential. In this analysis, a small positive trend was detected, by which larger uncaging potentials had stronger TTX effects, although the trend was not significant (Fig. 3*C2*; $P = 0.09$ amplitude, $P = 0.059$ area).

TTX Affects Spines of Different Neck Lengths. In our recent work, we found that the spine neck has a major role in filtering membrane potentials (22). This effect was bidirectional, occurring with uncaging potentials generated at the spine, but also, to a smaller extent, with somatic depolarizations, that invade the spine from the dendritic shaft. Given that layer 5 pyramidal neurons in mouse visual cortex have a population of spines with variable neck lengths (24), and that spines are heterogeneous in some of their functional characteristics (28), we wondered whether the amplification of uncaging potentials by sodium channels was specific to a particular type of spines. To test this, we examined the effect of TTX in spines of different neck lengths, using both 4- and 10-msec uncaging protocols (Fig. 4). In these paired experiments, for every spine, we measured the amplitude of the uncaging potential before and after addition of TTX, as a function of the spine neck length. With 4-msec uncaging protocols, we found that uncaging potentials in both short- and long-necked spines were similarly reduced by TTX (Fig. 4). The average amplitude of the uncaging potential was greatly modulated by the spine neck length, either in control conditions ($n = 19$ spines, $R = 0.65$; slope = −0.51 ± 0.13 mV/μm, $P < 0.001$), as found before (19), or in TTX (Fig. 4*B*; $n = 19$ spines, $R = 0.46$, slope = −0.26 ± 0.11 mV/μm, $P < 0.05$). The percent reduction in amplitude in TTX was comparable in spines of all different neck sizes, without any detectable correlation between the amount of reduction and the neck length (Fig. 2*B2*; slope = −8.31 ± 13.6, $R = 0.14$, $P = 0.55$). Similarly, in experiments with 10-msec uncaging pulses, no correlation was observed between the amount of reduction and neck length (data not shown; slope = 0.16 ± 12.3, $R = 0.005$, $P = 0.99$).

For both control and TTX experiments, pooled analyses from all spines examined (paired and unpaired experiments) showed a strong negative correlation between the spine neck length and the amplitude of the uncaging potential (for 4-msec events, $n = 76$ spines; $R = 0.73$, slope = −0.55 ± 0.06 mV/μm, $P < 0.001$ in control; $n = 48$ spines, $R = 0.52$; slope = −0.23 ± 0.05 mV/μm, $P < 0.001$ in TTX; for 10-msec events, $n = 15$ spines from 15 neurons, $R = 0.69$; slope = −1.45 ± 0.42 mV/μm, $P < 0.005$ in control standard artificial cerebrospinal fluid and $n =$

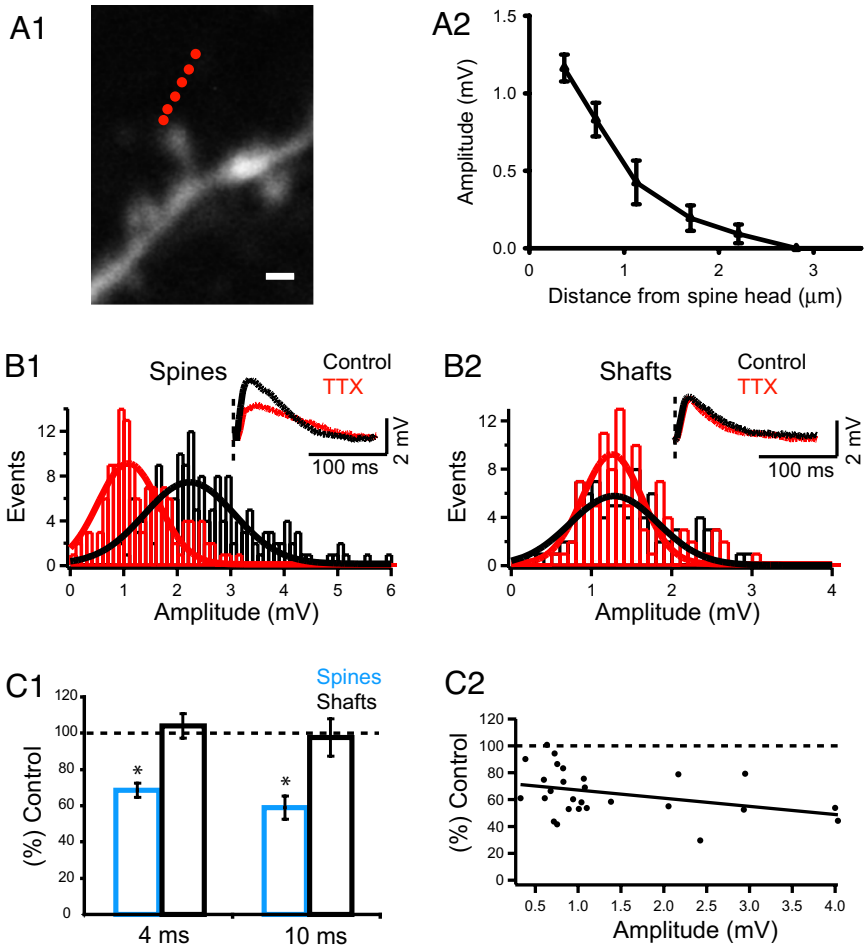

Fig. 3. TTX effect on uncaging potentials of different amplitudes. (*A*) Spatial resolution of 10-msec uncaging pulses. (*A1*) Red dots are site of uncaging in a spine at different distance from its head. (Scale bar, 1 μm.) (*A2*) Uncaging potential amplitude at different distances from the spine head (mean ± SD). (*B*) Histogram of all 10-msec uncaging potentials on spines (*B1*) and shafts (*B2*) in control and TTX. Note that, as in 4-msec uncaging pulses, a shift toward smaller potentials is caused by TTX in the distribution of spine but not shaft potentials. (*Inset*) Black (control) and red (TTX) traces correspond to an average of 10–15 depolarizations in a spine (*B1*) or shaft location (*B2*). (*C1*) Percentage amplitude from control in spines and shafts under 4- and 10-msec stimulation pulses. *, $P < 0.01$. (*C2*) Plot of the percentage amplitude from control after TTX vs. the amplitude of the uncaging potentials.

9 spines from nine neurons, $R = 0.51$; slope $= -0.51 \pm 0.32$ mV/μm, $P = 0.1$ in TTX). Interestingly, the slope (i.e., the attenuation of the potentials by the neck length) of the 10-msec uncaging events was steeper than that of the 4-msec events, as would be predicted from a larger synaptic conductance (8).

Taken together, these results confirm our past report of the inverse correlation between uncaging potential and neck length (19) and indicate that this relation is still present in TTX. Also, TTX appears to affect all spines equally, regardless of their spine neck.

Discussion

In this study, we investigate whether dendritic spines are excitable structures, a hypothesis suggested by theoretical studies (5, 7, 16, 17, 29, 30) and implied by our recent experimental results (18, 19), although never directly tested. Using two-photon glutamate uncaging, we find that uncaging potentials, as measured at the soma, are reduced by bath application of TTX if the uncaging is performed on spines but not if it is performed on dendritic shafts. The reduction of uncaging potential by TTX occurs with uncaging potentials of different amplitudes and in spines of different neck lengths. In fact, this effect is present in practically all spines examined (see paired experiments in Fig. 4).

The simplest interpretation of our data is that voltage-sensitive sodium channels are present in spines, and that they amplify uncaging potentials. Thus, our results confirm the hypothesis that dendritic spines are excitable structures, as originally proposed by Diamond *et al.* to explain their physiological results (5). Although structural confirmation of the existence of spine sodium channels in spines is still missing, proteomics studies have indeed identified sodium channel subunits as potential components of the postsynaptic density (31–33). In agreement with this, sodium imaging data have demonstrated sodium accumulation in dendritic spines during trains of backpropagating APs (ref. 34; H. D. Mansvelder and R.Y., unpublished results). Unfortunately, sodium transients in response to single APs could not be resolved, and sodium diffusion is fast, which makes it difficult to pinpoint the exact location of the sodium channels responsible for these accumulations.

We report a significant difference in the effect of TTX on uncaging potentials in dendritic spines or shafts, even when these locations are right next to each other (≈2 μm away). This differential effect of TTX further confirms that spines are electrically isolated by the spine neck (19) because if there were no electrical barrier between spines and shafts, there should not be any differences in their uncaging responses to bath application of TTX. In addition, the electrical filtering of the spine neck can help explain

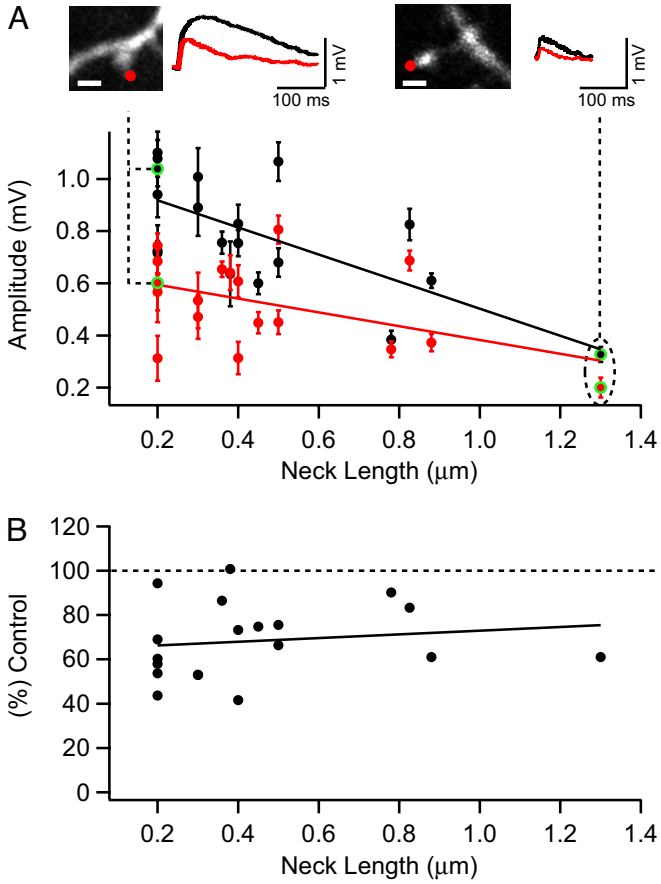

Fig. 4. TTX effect on spines of different neck lengths. (*A Upper*) Examples of uncaging potentials in spines with a short (*Left*) and long (*Right*) neck. Red dots are site of uncaging. Voltage traces under control (black) and TTX (red), corresponding to averages of 10–15 uncaging potentials for each spine. (Scale bar, 1 μm.) In both short- and long-necked spines, a reduction in the uncaging potential by TTX is evident. (*A Lower*) Plot of uncaging potentials amplitude vs. neck length from spines examined in both control and TTX conditions. Each point corresponds to average amplitude of the uncaging potential from each spine in control and TTX, including the standard error of each data point. Line is linear regression. Green points are paired experiments illustrated in *Upper*. (*B*) Percent amplitude from control uncaging potentials in TTX vs. neck length. Line is linear regression.

why TTX does not alter shaft-uncaging potentials, even though there is evidence, from cell-attached recordings, that functional sodium channels exist in dendrites of pyramidal neurons (26). It is likely that the local depolarizations attained after shaft uncaging are too small to significantly activate shaft sodium channels. Indeed, the responses to shaft uncaging measured at the soma are typically <1 mV and are similar in locations close to the soma where the electrical filtering because of the dendrite would be minimized (19). These dendritic depolarizations are too small to significantly activate sodium channels (35).

By the same reasoning, assuming the sodium channels in the spine and shaft have similar voltage dependencies, our data would imply that the depolarization in spines after spine uncaging must be large enough to significantly activate sodium channels. Given that the spine uncaging potentials, when measured at the soma, are also small (typically <2 mV for 4-msec uncaging pulses), these large spine depolarizations must be significantly filtered by the spine neck (19). In fact, one could argue that the functional reason for the amplification might be precisely to compensate for the spine neck filtering, and that this filtering would be necessary in the first place to prevent input interactions between excitatory inputs and help maintain a stable and linear dendritic integration arithmetic (22). Although we still do not have direct measurements of the membrane potential change evoked by the glutamate uncaging at the head of the spines, we expect it must be >10 mV, to significantly activate sodium channels (35). Indeed, that spine-uncaging potentials are affected by TTX, although they are too small at the soma to activate sodium channels, itself implies those sodium channels must be at the spine, and that the local depolarization they experience must be higher than the one measured at the soma. At the same time, this local depolarization cannot be large enough to trigger a local AP at the spine head, given that TTX only partially blocks the spine response. Even with the largest depolarizations, $\approx$50% of the uncaging potential still remains with blocked sodium channels.

Because sodium channels have a nonlinear voltage dependency, one would expect that increased spine depolarization should lead to an increased activation of sodium channels. To test this, we explored uncaging regimes that depolarized the spines more strongly. In these experiments, the uncaging potentials, indeed, became larger than expected, although the effect of TTX on these larger potentials was not significantly different from in the smaller depolarizations. Nevertheless, these comparisons should be interpreted with care because spines probably have potassium channels or other voltage-dependent conductances that could become activated by the glutamate uncaging, so different uncaging regimes may engage spine active conductances differently. Alternatively, it is possible that stimulation of a single spine is insufficient to fully engage spine sodium channels, but that simultaneous stimulation of many spines may be necessary to activate them fully. This joint stimulation of $\approx$20 spines could trigger a local AP in a segment of the dendrite (36).

The presence of sodium channels in the spines could explain why back-propagating APs in spines and shafts have similar amplitudes (18), despite the neck filtering (19), because spine sodium channels could fully regenerate the full-blown spike, even after its attenuation through the spine neck. Therefore, perhaps a function of the spine sodium channels is to ensure that the backpropagating AP can fully invade the spines, while leaving them isolated from excitatory postsynaptic potentials from other spines, something that could result in a more accurate learning rule. Moreover, by virtue of being clustered in spines, sodium channels could also significantly facilitate backpropagation, as illustrated in multicompartmental simulations where the same number of sodium channels has a stronger effect when they are clustered than if they are uniformly distributed along a dendrite (17). Consistent with the facilitatory effect of spines on backpropagation, we have detected several correlations between spine density and backpropagation efficiency (H. D. Mansvelder and R.Y., unpublished work).

Finally, we caution the reader that we have examined only uncaging potentials, and that it remains to be demonstrated by further experiments whether physiological excitatory postsynaptic potentials are also amplified by spine sodium channels. We think this is likely, given that spine uncaging potentials are similar in amplitude and kinetics to miniature postsynaptic potentials (19). In fact, the amplification of synaptic potentials by spine sodium channels could help explain the paradox of how subthreshold synaptic activation of individual spines can lead to calcium influx through NMDA receptors (NMDARs) (14, 37–39). If single-input synaptic potentials at the spine were similar to those measured in the dendritic shaft or soma (<2 mV under minimal stimulation conditions), they should not be able to activate NMDARs (40). That significant activation of NMDARs occurs when a single spine is activated synaptically (37–39) implies that physiological synaptic inputs must also give rise to a large depolarization at the spine and, moreover, because these depolarizations are small in somatic or dendritic recordings (38),

that they must also be filtered by the spine neck before they reach the dendrite.

Materials and Methods

Slice Preparation. All animal handling and experimentation were done according to National Institutes of Health guidelines. For the experiments on acute brain slices, 300-μm-thick coronal slices of visual cortex were prepared from postnatal day 13–16 C57BL/6 mice, as described (41). Animals were anesthetized with ketamine-xylazine (50 and 10 mg·kg^{-1}).

Imaging and Electrophysiology. All experiments were done at 37°C. Neurons were filled through the recording pipette with 200 μM Alexa 488 (Molecular Probes, Eugene, OR). Pipette solution contained 135 mM $KMeSO_4$, 10 mM KCl, 5 mM NaCl, 10 mM Hepes, 2.5 mM Mg-ATP, and 0.3 mM GTP, pH 7.3, with KOH. After cells were fully loaded with dye (5–30 min after break-in), dendritic location or spines was selected for imaging or uncaging. Electrophysiological recordings were performed in current– or voltage–clamp with whole-cell electrodes and Multiclamp 700b amplifiers (Axon Instruments, Sunnyvale, CA). Resting membrane potential was maintained at −65 mV. Imaging was done by using a custom-made two-photon laser-scanning microscope (23), consisting of a modified Fluoview (Olympus, Melville, NY) upright confocal microscope with a Ti:Sapphire laser (Chameleon; Coherent, Santa Clara, CA). A ×60/1.1 N.A. or a ×60/0.9 N.A. water-immersion objective (Olympus) was used. Unless mentioned otherwise, two-sided Student's *t* tests were used, and data are presented as mean ± SEM.

Two-Photon Uncaging of Glutamate. 4-Methoxy-7-nitroindolinyl-caged glutamate (2.5 mM; Tocris Cookson, Bristol, U.K.) was bath-applied, and a Lambda micropump (Bioptechs, Butler, PA) was used to control bath perfusion and minimize total bath volume. A custom-built two-photon microscope was controlled by custom software (42), and imaging and uncaging were performed at 725-nm excitation (Chameleon; Coherent). The laser was parked at a distance of ≈0.2 μm from spine heads or dendritic shafts of layer 5 pyramidal neurons that were filled with 200 μM Alexa 488 (Molecular Probes) through recording pipettes. Laser power was controlled by a Pockels cell (Conoptics, Danbury, CT), gated by square pulses (Master-8; AMPI, Jerusalem, Israel). For uncaging, laser pulses of 4–10 msec at 2-sec intervals were used with 25–30 mW of power on the sample plane. For imaging, 5–8 mW of laser power was used. Uncaging potentials were recorded from the soma in whole-cell current– or voltage–clamp by using standard electrophysiology equipment and analyzed off-line. TTX (Sigma, St. Louis, MO) was bath-applied at 1–5 μM. Image J (NIH, Bethesda, MD) was used to measure spine neck lengths, calculated from the proximal edge of the spine head to the edge of the dendrite, or by computing the shortest orthogonal distance between the base of the spine head and the edge of the dendrite. For spines with no discernible necks, we chose a minimum value of 0.2 μm.

We thank H. D. Mansvelder for observations and discussions that helped to initialize this project, G. Ellis-Davies (Drexel University College of Medicine, Philadelphia, PA) for initial samples of 4-methoxy-7-nitroindolinyl-glutamate and advice; A. Trevelyan, C. Stevens, C. Wilson, J. H. Goldberg, and P. Adams for helpful discussions; and members of the laboratory for comments. This work was funded by the National Eye Institute, the Pew Programs in the Biomedical Sciences, the Kavli Institute for Brain Science, and the New York STAR Center for High Resolution Imaging of Functional Neural Circuits. K.B.E. thanks the National Science Foundation for their support.

1. Ramón y Cajal S (1899) *La Textura del Sistema Nervioso del Hombre y los Vertebrados* (Moya, Madrid), Primera Edicion.
2. Gray EG (1959) *J Anat* 83:420–433.
3. Chang HT (1952) *Cold Spring Harbor Symp Quant Biol* 17:189–202.
4. Llinás R, Hillman DE (1969) in *Neurobiology of Cerebellar Evolution and Development*, ed Llinas R (American Medical Association Education and Research Foundation, Chicago), pp 43–73.
5. Diamond J, Gray EG, Yasargil GM (1970) in *Excitatory Mechanisms, Proc 5th Internation Meeting of Neurobiologists*, eds Andersen P, Jansen J (Universitets Forlaget, Oslo), pp 213–222.
6. Miller JP, Rall W, Rinzel J (1985) *Brain Res* 325:325–330.
7. Jack JJB, Noble D, Tsien RW (1975) *Electric Current Flow in Excitable Cells* (Oxford Univ Press, London).
8. Koch C, Poggio T (1983) *Proc R Soc London Ser B* 213:455–477.
9. Rall W, Segev I (1987) in *Synaptic Function*, eds Edelman GE, Gall WF, Cowan WM (Wiley, New York), pp 605–637.
10. Tsay D, Yuste R (2004) *Trends Neurosci* 27:77–83.
11. Wickens J (1988) *Prog Neurobiol* 31:507–528.
12. Koch C, Zador A (1993) *J Neurosci* 13:413–422.
13. Svoboda K, Tank DW, Denk W (1996) *Science* 272:716–719.
14. Yuste R, Denk W (1995) *Nature* 375:682–684.
15. Denk W, Sugimori M, Llinás R (1995) *Proc Natl Acad Sci USA* 92:8279–8282.
16. Segev I, Rall W (1988) *J Neurophysiol* 60:499–523.
17. Tsay D, Yuste R (2002) *J Neurophysiol* 88:2834–2845.
18. Nuriya M, Jiang J, Nemet B, Eisenthal KB, Yuste R (2006) *Proc Natl Acad Sci USA* 103:786–790.
19. Araya R, Jiang J, Eisenthal KB, Yuste R (2006) *Proc Natl Acad Sci USA* 103:17961–17966.
20. Canepari M, Nelson L, Papageorgiou G, Corrie J, Ogden D (2001) *J Neurosci Methods* 112:29–42.
21. Matsuzaki M, Ellis-Davies GC, Nemoto T, Miyashita Y, Iino M, Kasai H (2001) *Nat Neurosci* 4:1086–1092.
22. Araya R, Eisenthal KB, Yuste R (2006) *Proc Natl Acad Sci USA* 103:18779–18804.
23. Majewska A, Yiu G, Yuste R (2000) *Pflügers Arch* 441:398–409.
24. Benavides-Piccione R, Ballesteros-Yañez I, DeFelipe J, Yuste R (2002) *J Neurocytol* 31:337–346.
25. Lerma J (1997) *Neuron* 19:1155–1158.
26. Stuart GJ, Sakmann B (1994) *Nature* 367:69–72.
27. Hodgkin AL, Huxley AF, Katz B (1952) *J Physiol (London)* 116:424–448.
28. Yuste R, Majewska A, Holthoff K (2000) *Nat Neurosci* 3:653–659.
29. Baer SM, Rinzel J (1991) *J Neurophysiol* 65:874–890.
30. Shepherd GM, Brayton RK, Miller JP, Segev I, Rinzel J, Rall W (1985) *Proc Natl Acad Sci USA* 82:2192–2195.
31. Li KW, Hornshaw MP, Van der Schors RC, Watson R, Tate S, Casetta B, Jimenez CR, Gouwenberg Y, Gundelfinge ED, Smalla K-H, *et al.* (2004) *J Biol Chem* 279:987–1002.
32. Grant SGN, Husi H, Choudhary J, Cumiskey M, Blackstock W, Armstrong JD (2004) in *Excitatory-Inhibitory Balance, Synapses, Circuits, Systems*, eds Hensch TK, Fagiolini M (Kluwer/Plenum, New York), pp 13–44.
33. Yoshimura Y, Yamauchi Y, Shinkawa T, Taoka M, Donai H, Takahashi N, Isobe T, Yamauchi T (2004) *J Neurochem* 88:759–768.
34. Rose C, Kovalchuk Y, Eilers J, Konnerth A (1999) *Pflügers Arch* 439:201–207.
35. Stuart G, Sakmann B (1995) *Neuron* 15:1065–1076.
36. Losonczy A, Magee J (2006) *Neuron* 50:180–183.
37. Koester HJ, Sakmann B (1998) *Proc Natl Acad Sci USA* 95:9596–9601.
38. Yuste R, Majewska A, Cash S, Denk W (1999) *J Neurosci* 19:1976–1987.
39. Kovalchuk Y, Eilers J, Lisman J, Konnerth A (2000) *J Neurosci* 20:1791–1799.
40. Nowack L, Bregestovski P, Ascher P, Herbet A, Prochiantz A (1984) *Nature* 307:462–465.
41. Goldberg J, Tamas G, Aronov D, Yuste R (2003) *Neuron* 40:807–821.
42. Nikolenko V, Nemet B, Yuste R (2003) *Methods* 30:3–5.